On the upper limit for the energy of epithermal neutrons for Boron Neutron Capture Therapy

P. Torres-Sánchez, I. Porras, J. Praena, F. Arias de Saavedra and M.P. Sabariego

Departamento de Física Atómica, Molecular y Nuclear
Facultad de Ciencias, Universidad de Granada,
E-18071, Granada, Spain

Abstract

The upper limit of the energy for epithermal neutrons is usually fixed to 10 keV based on the experience with spectra from reactors used until now for Boron Neutron Capture Therapy. The future use of accelerators with this therapy will provide different neutron spectra that require a more detailed study of this upper limit. Using our own Monte Carlo neutron transport code, we have calculated figures of merit on the dose depth profile to find this upper limit. Our results indicate that this upper limit could be incremented up to 17 keV under these new conditions.

Keywords: BNCT, accelerators, dose depth profile, Monte Carlo simulations

1. Introduction

Boron Neutron Capture Therapy (BNCT) is facing a new era in the next years. First, due to the progress in the new accelerator-based neutron sources (ABNS) which can be built in hospitals and are expected to make this therapy more easily available (Green, 1998; Lennox, 2001; Kreiner et al., 2016). Second, the very promising results obtained in the most recent clinical trials (Barth et al., 2012) in other than brain tumors, as head and neck cancers (Kato et al., 2004; Kankaanranta et al., 2012), open the way to new applications of BNCT.

The ABNS are expected to have substantially different neutron spectra from the reactor-based ones, with which all previous clinical trials have been done.

The neutron energy is the key for the therapeutic ability of a BNCT treatment. Epithermal neutron sources, on the keV range, have been successfully used in the clinical trials with research reactors. Currently the recommendations of the IAEA for a neutron beam for BNCT (IAEA TECDOC, 2001) establish a limit for the fast neutron component which, by definition, includes all neutrons above 10 keV.

The upper limit of 10 keV for epithermal neutrons it is not a precise value, being rather arbitrary. A more precise determination has some little effects for reactor-based sources. The reason of this limiting value is to reduce the high energy tail of the neutron spectrum, which usually goes up to 1 MeV. However, for an accelerator-based neutron source, where the maximum energy can be adjusted by kinematics and can be much lower, and for which the maximum of the neutron spectra can be near 10 keV, the establishment of a limiting value for the epithermal part of the spectrum (which should account for more than 90% of the flux) is critical. For example, some proposed accelerator-based beams obtained from the $^7\mathrm{Li}(p,n)$ reaction with different moderators present a maximum in the neutron fluence between 10 and 20 keV (Bleuel et al., 1998). Other studies on ABNS consider as the epithermal neutron energy upper limit values of 40 keV (Faghihi and Khalili, 2013) or 50 keV (Bisceglie, 2000).

It is clear from previous studies (Bisceglie et al., 2000) that the optimal energy of neutrons for the treatment of deep seated tumors is of the order of a few keV. However, monoenergetic neutrons are not possible and, in order to obtain an optimal realistic beam, lower and higher energies are going to be present in the beam. The requirements for beam quality (IAEA TECDOC, 2001) are expressed in terms of the epithermal neutron fluence, defined in this document as the fluence for the energy range from 0.5 eV to 10 keV. For example, the desirable minimum beam intensity would be 10^9 epithermal neutrons cm^{-2} s^{-1}, the fast neutron dose component as well as the dose from gamma contamination of the beam should be below 2×10^{-13} Gy cm^2 per epithermal neutron, and the ratio of thermal flux to epithermal flux should be less than 0.05. Therefore, these beam parameters depend crucially on the range for the neutron energy established for being considered epithermal neutrons.

In phantom figures of merit (FOM) have been proposed as a better reference for beam quality (Wallace et al., 1994; Bleuel et al., 1998). The most used are: the advantage depth x_{AD} (usually denoted AD in the literature), which is the depth where the tumor dose equals the maximum normal tissue dose; and the therapeutic range, which is an interval x_{TR1}, x_{TR2} in which the tumor dose is at least twice the maximum dose in normal tissue.

The goal of this work is to analyze the dependence of the FOM and other depth dose parameters in terms of the neutron energy. This type of analysis depends crucially on the geometry and composition of the tissues as well on some parameters for the equivalent weighted dose which are: the relative biological effectiveness (RBE) for the different dose components, and the ^{10}B concentration both at the tumor and at healthy tissue. Previous studies that have been performed using Monte Carlo calculations (Wallace et al. 1994, Biscegle et al., 1888) for the treatment of brain tumors, with a geometry model of the skull and brain. As BNCT is facing new applications, such as head and neck cancers and other soft tissue tumors, we have adopted a different reference non-specific phantom for this work which will be discussed in the next section.

Another aim of this work is to describe the depth dose curves by a fit to simple mathematical formulas. In this way, the calculations for different RBE and/or boron concentrations at tumor and at tissue can be performed in a straightforward way from the tabulated coefficients that will be presented below.

2. Methods

In order to perform fast computations of the depth dose functions, we have developed our own Monte Carlo neutron transport code called NeuTrans, which has been specifically designed for the given geometry and composition. For this reason, it is much faster than a general purpose Monte Carlo code as MCNP. An unidirectional monoenergetic neutron beam of 5 cm radius is transported into a 10 cm radius, 10 cm height cylinder composed of a standard soft tissue, the ICRU 4-component tissue (ICRU Report, 1992). Its mass composition is ^{1}H: 0.101172, ^{12}C: 0.111000, ^{14}N: 0.02600 and ^{16}O: 0.761828. In this code, the neutron moderation has been modeled concerning the main interactions of neutrons with tissue such as elastic collisions and also ^{14}N capture and ^{1}H radiative capture. In the event of any interaction, the energy delivered by the neutron (for elastic collisions) or the products of reaction in capture has been recorded in boxes arranged on a grid through the material. In order to achieve a reduced execution run time, a technique of convolution has been used. Namely, a punctual neutron beam was directed into the center of the cylinder, and the total dose produced by this beam was recorded on the whole grid. Subsequently, this dose map was convolved according to the spatial structure of the beam to finally obtain the dose in the axis of the cylinder. The size of the region in which data was recorded has been set large enough so that the effect of the systematic loss of information in the borders of the cylinder was negligible at the cylinder axis, where the data of interest was computed. The computation of the photon dose required special attention due to its deposition far from the position where the photon creation occurred. In this case, a semi-empiric model of the photon dose deposition was applied (Sabariego et al. 2008). This model takes into account two types of dose, the direct dose produced by primary photons, and the dose produced by scattered photons, as shown in equation 1,

$$D_\gamma\left(\vec{r}_k\right) = \frac{1}{4\pi\rho}\sum_j n_j \frac{e_0\left(\left|\vec{r}_j - \vec{r}_k\right|\right) + e_s\left(\left|\vec{r}_j - \vec{r}_k\right|\right)}{\left|\vec{r}_j - \vec{r}_k\right|^2}\,, \tag{1}$$

where a sum on the boxes is included. In the j-th box, n_j photons have been created and it is centered at $\vec{r}_j$, ρ is the density of the medium and $e_0(r)$ and $e_s(r)$ are given by:

$$e_0\left(r\right) = \begin{cases} A_0\left(1 - e^{-\mu_0 r}\right) & r \leq R_0 \\ A_0 e^{-\mu_0 r}\left(e^{\mu_0 R_0} - 1\right) & r > R_0\,, \end{cases} \tag{2}$$

$$e_s\left(r\right) = C_1\left(\mu_1\right)^2 r e^{-\mu_1 r} + C_2\left(\mu_2\right)^3 r^2 e^{-\mu_2 r}\,, \tag{3}$$

where the parameters used in these formulas for the 2.224 keV photons from the hydrogen capture were obtained by fitting Monte Carlo simulation calculations

<table>
<tr><th></th><th>ω_t</th><th>ω_f</th><th>ω_γ</th><th>ω_B</th><th>$\chi_B(ppm)$</th><th>r_B</th></tr>
<tr><td>Healthy tissue</td><td rowspan="2">3.2</td><td rowspan="2">3.2</td><td rowspan="2">1.0</td><td>3.8</td><td>10</td><td rowspan="2">0.422</td></tr>
<tr><td>Tumor</td><td>1.3</td><td>35</td></tr>
</table>

Table 1: RBE factors, the boron concentration in healthy tissue and tumor and the effective ponderation factor that has been used in the estimations of the total dose.

(Sabariego 2016).

Furthermore, the dose has been split in thermal, proton-recoil or fast and photon dose (Goorley et al. 2002). The corresponding RBE factor has been applied to each of them, and the boron contribution, which is proportional to thermal dose, has been included as in equation 4

$$D = (\omega_t + \omega_B \chi_B r_B) D_t + \omega_f D_f + \omega_\gamma D_\gamma \, . \tag{4}$$

The values for the weights ω_x, the boron concentration, χ_B, and the effective ponderation factor, r_B, can be found in Table 2.

Our code has been validated against MCNPX revealing minor discrepancies, below the 5% of error demanded for dosimetry measurements on clinical treatments. This validation has been made for the axis of the cylinder and the total physical dose received on tissue. The validation at 15 keV can be seen in Figure 1.

Several runs of the developed code have been made for energies of the initial monoenergetic beam, in the range 0.1 to 40 keV. The in-depth dose profile for each part of the dose has been fit in terms of the depth in tissue and the energy of the beam, following the expressions 5, 6 and 7.

$$D_t\left(E,x\right) = a_t\left(E\right) + b_t\left(E\right)x + c_t\left(E\right)x^2 + d_t\left(E\right)x^3 + e_t\left(E\right)x^4 \, , \tag{5}$$

$$D_f\left(E,x\right) = \left(a_f\left(E\right) + b_f\left(E\right)x\right) \cdot e^{-c_f(E)x} \, , \tag{6}$$

$$D_\gamma\left(E,x\right) = \left(a_\gamma\left(E\right) + b_\gamma\left(E\right)x\right) \cdot e^{-c_\gamma(E)x - d_\gamma(E)x^2} \, . \tag{7}$$

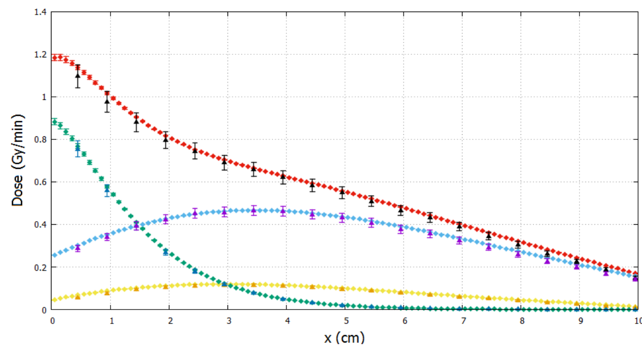

Figure 1: NeuTrans vs. MCNPX comparison and validation for three parts of the dose and the total dose. The diagram shows the comparison at 15 keV, in the center of the interval of energies of interest. The colors for the dose results are: black for total, brown for thermal, dark blue for fast and purple for photon in the case of MCNPX and red for total, yellow for thermal, green for fast and light blue for photon in the case of NeuTrans. All the parts of the dose keep within the 5 % error.

Where all the energy-dependent functions shown are defined in terms of coefficients to be fitted in the following equations

$$\alpha_t(E) = \alpha_{t0} E^{\alpha_{t1}} \qquad \alpha = a, b, c, d, e \tag{8}$$

$$\beta_f(E) = \beta_{f1} E + \beta_{f2} E^2 \qquad \beta = a, b \tag{9}$$

$$c_f(E) = c_{f0} E^{c_{f1}} \cdot e^{-c_{f2} E} \tag{10}$$

$$\mu_\gamma(E) = (\mu_{\gamma 0} + \mu_{\gamma 1} E) E^{\mu_{\gamma 2}} \qquad \mu = a, b, c \tag{11}$$

$$d_\gamma(E) = (d_{\gamma 0} + d_{\gamma 1} E) \cdot E^{d_{\gamma 2}} + d_{\gamma 3}\,. \tag{12}$$

3. Results

The fit of the equations for all the simulated energies lead to a set of parameters for this actual geometry and tissue, that could be made extensive to others easily. For this one, the values of the parameters are given in Table 2.

Using these parameters, the behavior of the different parts of the dose has been analyzed as a function of the energy. This can be seen in Figure 2. The thermal dose has a maximum around 2 to 4 cm from the surface, and its effect

$a_{t0} = 0.06087(17)$	$a_{t1} = -0.1347(12)$	$b_{t0} = 0.08679(17)$	$b_{t1} = -0.1282(10)$
$c_{t0} = -0.02550(8)$	$c_{t1} = -0.1848(18)$	$d_{t0} = 2.464(13) \cdot 10^{-3}$	$d_{t1} = -0.238(3)$
$e_{t0} = -8.32(6) \cdot 10^{-5}$	$e_{t1} = -0.280(5)$		
$a_{f1} = 0.06678(12)$	$a_{f2} = -3.80(24) \cdot 10^{-4}$	$b_{f1} = 0.05637(15)$	$b_{f2} = -2.2(3) \cdot 10^{-4}$
$c_{f0} = 1.1668(7)$	$c_{f1} = -5.7(4) \cdot 10^{-3}$	$c_{f2} = 2.67167(20) \cdot 10^{-3}$	
$a_{\gamma 0} = 0.315302(14)$	$a_{\gamma 1} = 1.79(16) \cdot 10^{-4}$	$a_{\gamma 2} = -0.0864(3)$	
$b_{\gamma 0} = 0.2157(3)$	$b_{\gamma 1} = -1.9(3) \cdot 10^{-4}$	$b_{\gamma 2} = -0.16719(10)$	
$c_{\gamma 0} = 0.1388(4)$	$c_{\gamma 1} = -1.83(5) \cdot 10^{-3}$	$c_{\gamma 2} = -0.1709(21)$	
$d_{\gamma 0} = -0.01024(22)$	$d_{\gamma 1} = 4.38(12) \cdot 10^{-5}$	$d_{\gamma 2} = -0.1196(24)$	$d_{\gamma 3} = 0.0233(23)$

Table 2: Fit parameters for each part of the dose and for ICRU-4 tissue and cylindrical geometry. The parameters have been obtained using a least squares fit.

reduces with the energy of the monoenergetic beam as less neutrons are capable to thermalize before leaving the tissue. The photon dose behaves in a similar way, but affects a wider region in tissue due to the at-distance photon energy deposition. On the other hand, the proton-recoil dose has a bigger impact on the surface of the tissue, and its magnitude increases almost linearly with the energy of the neutron beam. This is the part of the dose that will make the limitation of the effectiveness of BNCT.

To help defining this upper limit of the neutron energies for BNCT with some accuracy, some Figures Of Merit (FOM) can be used:

1. Depth at which the maximum dose in healthy tissue is reached, x_H.
2. Maximum dose in healthy tissue, $D_{H,Max} = D_H(E, x_H)$. This FOM is of special interest as it establishes the total irradiation on the treatment.
3. Depth at which the maximum dose in tumor is reached, s_T.
4. Maximum Dose in tumor, $D_{T,Max} = D_T(E, x_T)$.
5. Advantage depth (AD). It is the distance at which the dose in tumor matches the maximum dose in healthy tissue, and indicates the maximum depth at which treatments are applicable.
6. Therapeutic range (TR). Its the depth interval (TR1-TR2) at which the

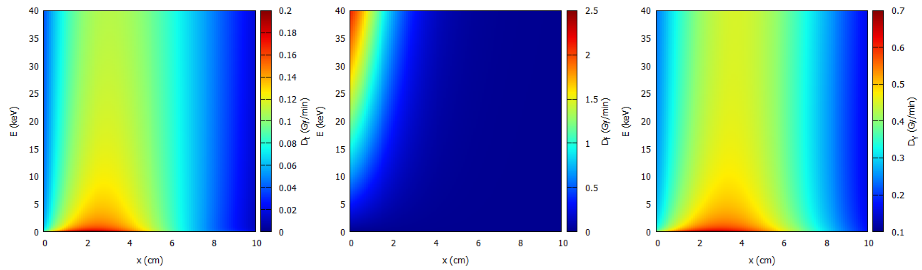

Figure 2: Energy-depth plots for the three parts of the dose. Thermal dose is shown on the left, proton recoil dose on the center and photon dose on the right. Depth in tissue is placed in the horizontal axis and energy in the vertical axis in linear scale. Dose is indicated with the color code next to each plot. Color scales are not the same for the three diagrams.

dose in tumor is at least twice as much as the maximum dose in healthy tissue, and reflects the region in which the treatment can be fully effective.

The values of the FOM for monoenergetic neutron beams in the energy range of 0.1 to 40 keV can be found in Table 3. In addition, Figure 3 shows the tumor dose as a function of the depth in tissue and the neutron energy, together with the AD, TR and x_T. Besides, some other quantities of interest are the energy at which both the AD and TD are the largest, which is $E = 3.5$ keV, the energy at which the therapeutic range ceases to exist, at $E = 17.3$ keV. Another fact is that the maximum dose in the tumor has a minimum at $E = 15.9$ keV, and then starts to grow again due mainly to the fast dose. In addition, the AD does not have a sharp end, but it slows down almost linearly as energy is increased.

Although the energy of the best performance of BNCT has been shown to be in the region of the few keV, namely 3.5 keV, it keeps being acceptable to use in a broader range of energies. It is of special relevance that there is not a sharp limit on AD. This makes the setting of the limit on 10 keV as relatively arbitrary. The utilization of other FOM helps to confirm that neutrons with energies up to 15 - 18 keV or even 20 keV are also suitable for BNCT.

This makes more evident the fact that it is necessary to establish the upper limit of neutron energy with some care so that neutrons that could be appropriate for being used on BNCT are not rejected due to arbitrary reasons. Another

E (keV)	$D_{H,Máx}$ $\left(\frac{\text{Gy}}{\text{min}}\right)$	x_H (cm)	$D_{T,Máx}$ $\left(\frac{\text{Gy}}{\text{min}}\right)$	x_T (cm)	x_{AD} (cm)	x_{TR_1} (cm)	x_{TR_2} (cm)
0.1	2.3318	2.2748	12.0670	2.2113	9.0253	0	6.7835
1	1.9283	2.4945	9.7108	2.5092	8.8568	0	7.2192
2	1.8462	2.4091	9.1260	2.5848	8.9252	0	7.3415
5	1.8810	1.0077	8.4649	2.6312	8.9398	0	7.3005
10	2.6950	0.0018	8.0997	2.5433	8.2452	0.1421	5.9703
12	3.0621	0.0	8.0382	2.4737	7.9291	0.3267	5.3153
14	3.4217	0.0	8.0048	2.3859	7.6202	0.5901	4.5784
16	3.7732	0.0	7.9948	2.2748	7.3163	1.0546	3.6336
18	4.1163	0.0	8.0065	2.1368	7.0184	–	–
20	4.4505	0.0	8.0405	1.9635	6.7255	–	–
25	5.2465	0.0	8.2428	1.3690	6.0028	–	–
30	5.9846	0.0	8.6262	0.8893	5.2826	–	–
40	7.2719	0.0	9.5952	0.5389	3.8580	–	–

Table 3: Values for the main FOM for the depth dose profile in BNCT in the analyzed energy range. Maximum dose $D_{X,Máx}$ in healthy tissue $X = H$ and tumor $X = T$ and their depth x_X are included together with AD and TD1-TD2.

solution could be to fix the limit differently according to the specific shape of the neutron spectrum, worrying instead only on that some requirements of the actual in-depth dose profile may have. This solution would also profit from having the type of tumor and its shape and position in tissue in consideration.

4. Conclusions

In this work, analytical simple forms for the different contributions of the dose in Boron Neutron Capture Therapy with epithermal neutrons are given. This allows us to perform in a very fast way calculations of the total depth dose profile and the figures of merit for different values of the boron concentration and/or the RBE factors.

The application of these formulas to the analysis of the behavior of the

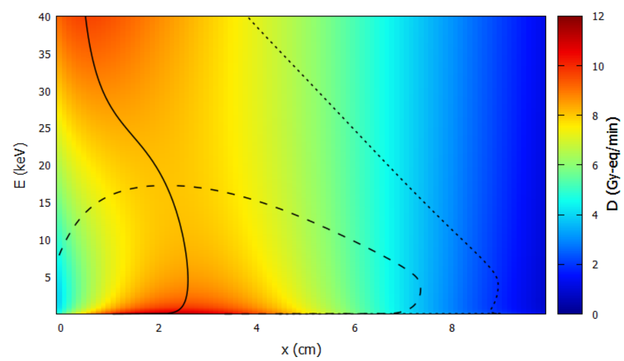

Figure 3: Energy-depth plot for the total dose in tumor. Depth in tissue is placed in the horizontal axis and energy in the vertical axis in linear scale. Dose is indicated with the color code next to each plot. Together with the color plot, the variation with energy of the main FOM is indicated with lines. Maximum dose in the tumor is indicated with a solid line, AD with a dotted line and TR1-2 with a dashed line

different figures of merit with respect to the neutron energy shows that, for a cylindrical phantom of ICRU 4-component soft tissue, up to 17.3 keV, there exists a range where the tumor dose exceeds twice the maximum dose in healthy tissue. For this reason we conclude that limiting the energy range up to 10 keV is a too stringent criterion for a therapeutic beam suitable for BNCT, and raising this limit at least to 17.3 keV should be considered. This is specially important for accelerator-based neutron sources which may have the maximum of the spectrum in the keV range.

References

Barth, R.F., Vicente, M.G.H., Harling, O.K., Kiger III, W.S., Riley, K.J., Binns, P.J., et al., 2012. Current status of boron neutron capture therapy of high grade gliomas and recurrent head and neck cancer. Radiat. Oncol. 7, 46.

Bisceglie B.E., P Colangelo P., N Colonna N., Santorelli P. and Variale V., 2000. On the optimal energy of epithermal neutron beams for BNCT. Phys. Med. Biol. 45, 49–58.

Faghihi F. and Khalili S., 2013. Beam shaping assembly of a DT neutron source for BNCT and its dosimetry simulation in deeply-seated tumor. Radiat. Phys. Chem. 51 (4-6), 561–569.

Goorley J.T., Kiger W.S. and Zamenhof R.G., 2002. Reference dosimetry calculations for neutron capture therapy with comparison of analytical and voxel models. Med. Phys., 29, 145156.

Green, S., 1998. Developments in accelerator based boron neutron capture therapy. Radiat. Phys. Chem. 51 (4-6), 561–569.

IAEA TECDOC, 2001. Current status of neutron capture therapy. TEC-DOC1223. International Atomic Energy Agency.

ICRU Report, 1992. Report 46: Photon, Electron, Proton and Neutron Interaction Data for Body Tissues. International Commission on Radiation Units and Measurements, Bethesda, MD.

Kankaanranta L., Seppala, T. Koivunoro H. et al., 2012. Boron neutron capture therapy in the treatment of locally recurred head-and-neck cancer: final analysis of a phase I/II trial. Int. J. Radiat. Oncol. Biol. Phys. 82, e67-75.

Kato I., Ono K., Sakurai Y. et al., 2004. Effectiveness of BNCT for recurrent head and neck malignancies. Appl. Radiat. Isot. 61, 1069-1073 (2004).

Kreiner AJ, Bergueiro J, Cartelli D et al. 2016. Present status of Accelerator-Based BNCT. Rep Pract Oncol Radiother. 21, 95-101.

Lennox, A.J., 2001. Accelerators for cancer therapy. Radiat. Phys. Chem. 61, 223-226.

Sabariego, M.P., 2016. Modelo semianalítico para cálculos de dosimetría en radioterapia. PhD thesis, Universidad de Granada. ISBN: 978-84-9125-754-7. URL: http://hdl.handle.net/10481/43469

Sabariego M.P., Porras I. and Lallena A.M., 2008. Simple analytical expressions for the dose of point photon sources in homogeneous media. Phys. Med. Biol. 53, 6113-6128, corrigendum 54, 4623 (2009).

Wallace S.A., Mathur J.N. and Allen B.J., 1994. Treatment planning figures of merit in thermal and epithermal boron neutron capture therapy of brain tumours, Phys. Med. Biol. 39, 897–906.